Original Article

PIEZO1 activation enhances myogenesis and mitigates muscle degeneration in rotator cuff tear

Tihui Wang [a, b, 1], Shujing Feng [c, 1], Hao Zhou [c, 1], Wenhua Mao [e], Ruijun Bai [d], Yuan Xia [a], Jianghu Huang [a], Rui Zhang [a, *], Feiyue Lin [a, f, **]

[a] Department of Orthopaedics, Shengli Clinical Medical College of Fujian Medical University, Fuzhou, 350001, China
[b] Department of Orthopaedics, Mindong Hospital Affiliated to Fujian Medical University, Ningde, 355000, China
[c] Department of Sports Medicine, School of Exercise and Health, Shanghai University of Sport, Shanghai, 200438, China
[d] Department of Orthopaedics, Wuxi Ninth People's Hospital, Soochow University, Wuxi, 214000, China
[e] XianJu People's Hospital, Zhejiang Southeast Campus of Zhejiang Provincial People's Hospital, Affiliated Xianju's Hospital, Hangzhou Medical College, Xianju, Zhejiang, China
[f] College of Clinical Medicine for Oncology, Fujian Medical University, China

ARTICLE INFO

ABSTRACT

Muscle degeneration is a common issue caused by rotator cuff tear (RCT) which significantly affects prognosis. Muscle stem cells (MuSCs) play a crucial role to prevent muscle degeneration after RCT. However, the pathological changes and detailed molecular mechanism underlying the myogenesis of MuSCs after RCT remain incomplete. The current study established single-cell landscape of supraspinatus muscles and found decreased expression of PIEZO1 and impaired myogenic potential of MuSCs from RCT patients. Reduced expression of PIEZO1 impaired the myogenesis of MuSCs by inhibiting the ERK/MAPK pathways. Furthermore, selective PIEZO1 agonist Yoda1 had the potential to alleviate muscle degeneration and improve shoulder function following RCT. This study emphasized the role of PIEZO1 in the myogenesis of MuSCs and suggested that activating PIEZO1 could be a potential non-surgical treatment option to reduce muscle degeneration after RCT.

1. Introduction

Rotator cuff tear (RCT) is a common musculoskeletal condition that causes shoulder pain and disability, affecting about 22.1 % of the general population [1]. Although surgical repair is a primary treatment for severe RCT, its effectiveness is often disappointing. Studies have shown that the retear rate after RCT repair can be as high as 94 %, largely due to significant muscle degeneration including muscular atrophy, fatty infiltration and fibrosis [2—4].

Especially, it severely impairs muscular function in RCT patients, reduces the success rate of surgery, and accelerates the progression to irreversible RCT [4]. Therefore, understanding the complex mechanisms behind muscle degeneration following RCT is crucial for developing effective treatment strategies.

Muscle stem cells (MuSCs), also known as satellite cells, are a group of stem cells situated between the basement membrane and the fibrous plasma membrane [5—7]. Under normal conditions, MuSCs remain quiescent but become activated in response to external stimuli affecting skeletal muscle. Once activated, MuSCs begin their myogenic program, entering the cell cycle to proliferate, differentiating, and ultimately forming new skeletal muscle fibers or fusing with existing ones [8]. Thus, these cells have the potential for myogenic differentiation, playing a crucial role to prevent muscle degeneration after RCT. However, the pathological changes and detailed molecular mechanism underlying the myogenesis of MuSCs after RCT remain incomplete.

RCT is marked by painful limitations in range of motion and presents a significant clinical challenge for orthopedic surgeons [9].

* Corresponding author. No. 134, East Street, Gulou District, Fuzhou City, Fujian Province, 350001, China.
** Corresponding author. No. 134, East Street, Gulou District, Fuzhou City, Fujian Province, 350001, China.
E-mail addresses: zhangruisl@outlook.com (R. Zhang), linfeiyue@sina.com (F. Lin).

Peer review under responsibility of the Japanese Society for Regenerative Medicine.
[1] These authors contributed equally to the current study.

Previous researches have shown that RCT could impair the biomechanical balance of the shoulder, thereby decreasing the mechanical stimuli transmitted to skeletal muscles via the tendon [10]. Mechanical force is essential for maintaining muscular quality [7]. However, it is still unclear whether mechanical stimuli play a role in mediating myogenesis of MuSCs following RCT.

In this study, we established single-cell landscape of supraspinatus muscles and found decreased expression of PIEZO1 and impaired myogenic potential in MuSCs from RCT patients. Reduced expression of PIEZO1 impaired the myogenesis of MuSCs by inhibiting the ERK/MAPK pathways. Furthermore, selective PIEZO1 agonist Yoda1 had the potential to alleviate muscle degeneration and improve shoulder function following RCT. This study emphasized the role of PIEZO1 in the myogenesis of MuSCs and suggested that activating PIEZO1 could be a potential non-surgical treatment option to reduce muscle degeneration after RCT.

2. Results

2.1. Single-cell RNA sequencing revealed decreased differentiation potential and mechanical stimulus response in supraspinatus MuSCs after rotator cuff tear

To investigate the mechanism of muscular degeneration after RCT, we first collected discarded supraspinatus muscles from individuals with or without RCT for single-cell RNA sequencing. In the scRNA-seq analysis, cells were categorized into 8 clusters including endothelial cells, FAP cells, macrophages, muscle stem cell, smooth muscle cells, T/NK cells, tenocytes (Fig. 1a and b). Due to the crucial role of MuSCs in muscle degeneration, we mainly focused on this cluster which highly expressed Pax7, MYF5 (Fig. 1b). Further Gene Ontology (GO) enrichment analysis of significantly downregulated genes of MuSCs in RCT groups indicated that cell differentiation and cell response to mechanical stimulus were suppressed (Fig. 1c). Thus, the scRNA-seq data indicated MuSCs in rotator cuff muscle might suffer decreased differentiation potential and mechanical stimulus response after RCT.

2.2. There were decreased myogenic differentiation ability and reduced expression of PIEZO1 in supraspinatus MuSCs after rotator cuff tears

To confirm the finding from scRNA-seq data, fluorescence-activated cell sorting (FACS) was used to firstly purify MuSCs in supraspinatus muscle from individuals with rotator cuff tear (RCT) and control groups (Fig. 2a). Marker gene PAX7 was analyzed using immunofluorescence staining, revealing almost all the obtained cells were PAX7 positive MuSCs (Fig. 2b and c). Then the myogenic differentiation ability of MuSCs were investigated. Following myogenic induction, immunofluorescence staining of myogenic differentiation marker MYHC showed significantly decreased myofiber fusion rate in MuSCs from patients with RCT (RCT group) when compared those from control patients without RCT (CTRL group) (Fig. 3a and b). RT-qPCR results also demonstrated significantly lower expression levels of myogenic markers (MYH1, MYOG, MCK) in the RCT group compared to controls, indicating reduced myogenic differentiation potential in MuSCs from RCT group (Fig. 3c). Furthermore, since the ion channel PIEZO plays an important role in translating mechanical forces into intracellular signals and further biological effects [7], decreased mechanical stimulus response enriched in scRNA-seq data indicated potential changes in PIEZO expression. There wasn't statistic significance discovered in the expression of Piezo2 between RCT and CTRL group (Fig. 3d). However, both gene and protein expression levels of PIEZO1 were found significantly decreased in the RCT group

compared to controls, suggesting altered mechanosensitive channels in muscle cells after RCT (Fig. 3d and e). Taken together, MuSCs from patients with RCT exhibited impaired myogenic differentiation potential and reduced expression of PIEZO1.

2.3. Ablation of Piezo1 in MuSCs led to decreased myogenic differentiation ability

To investigate the role of Piezo1 in myogenic differentiation potential of MuSCs, we generated a MuSCs-specific Piezo1 conditional knockout (KO) mouse model by crossing Pax7-CreERT2 and Piezo1 flox/flox (f/f) mice. Following tamoxifen induction, Piezo1 KO MuSCs were isolated, and the efficiency of Piezo1 knockout was confirmed by RT-qPCR for gene expression and Western blot for protein levels (Fig. 4a and b). Immunofluorescence staining for myogenic differentiation marker MYHC showed significantly decreased myotube fusion rate in Piezo1 KO MuSCs, indicating impaired myogenic differentiation potential (Fig. 4c and d). Gene expression analysis of myogenic markers (MYH1, MYOG, MCK) further supported these findings, showing markedly decreased expression levels in Piezo1 KO MUSCs compared to controls (Fig. 4e). These collective evidences underscored that Piezo1 deficiency in MuSCs led to impaired myogenic differentiation capacity.

2.4. PIEZO1 regulated myogenic differentiation of MuSCs by MAPK pathways

To further explore the mechanism of how PIEZO1 regulate myogenesis of MuSCs, the mRNA-seq was firstly performed to obtain differently expressed genes between MuSCs isolated from patients with RCT (RCT group) or control patients without RCT (CTRL group). We noticed the KEGG analysis enriched MAPK signaling pathway (Fig. 5a). This enrichment term suggested PIEZO1 might regulate myogenic differentiation of MuSCs through MAPK pathways.

Subsequently, healthy human MuSCs were treated with Piezo1 agonist Yoda1 and Piezo1 inhibitor GsMTx4, respectively. Western blot analysis showed activation of Piezo1 significantly increased the phosphorylation of MEK/ERK protein levels, while inhibitor treatment suppressed their activation (Fig. 5b). Thus, Piezo1 could influence downstream activity of MAPK signaling. To further investigate the biological effects of MAPK in myogenesis of MuSCs, MAPK agonist TBHQ and MAPK inhibitor U0126 were used during myogenic differentiation of MuSCs.

Immunofluorescence staining for MYHC revealed enhanced myogenic differentiation ability after treatment with MAPK agonist TBHQ and reduced myogenic differentiation ability after treatment with MAPK inhibitor U0126 (Fig. 5c and d). Furthermore, gene expression analysis demonstrated a consistent trend with the result of MYHC immunofluorescence staining, where TBHQ treatment upregulated myogenic marker genes (e.g., MYH1, MYOG, MCK), while U0126 treatment led to their downregulation (Fig. 5e). Thus, MAPK could effectively regulate the myogenic differentiation ability of MuSCs.

Taken together, these findings suggested that Piezo1 regulated myogenic differentiation of MuSCs by MAPK pathways, highlighting the critical role of Piezo1 in preventing muscle degeneration after RCT.

2.5. Yoda1 could alleviate the muscle degeneration and enhance the shoulder function in RCT model

According to aforementioned data, activating Piezo1 of MuSCs might be a potential strategy to prevent muscle degeneration after RCT. To explore the rescue effects, MuSCs from RCT patients were
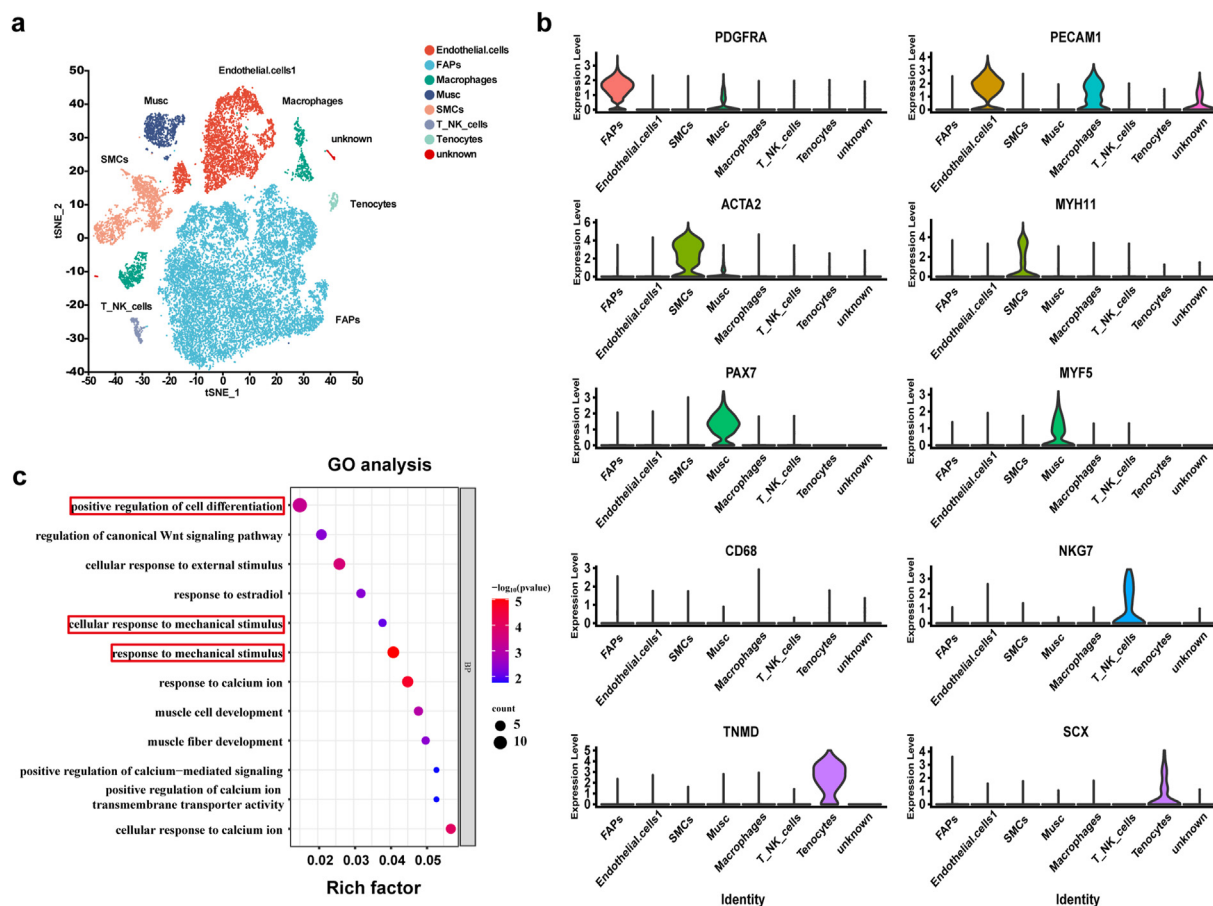
Fig. 1. Single-Cell RNA Sequencing revealed decreased differentiation potential and mechanical stimulus response in supraspinatus MuSCs after rotator cuff tear. a. The UMAP plots of cell clusters. Discarded human samples isolated from supraspinatus muscle tissues with or without rotator cuff tears were obtained during surgery and subsequent scRNA-seq was performed. A total of 22858 cells were finally clustered into 8 groups. b. Violin plots of representative marker genes expressed in different cell clusters. c. Gene Ontology enrichment analysis of significantly downregulated genes of MuSCs in RCT groups.

induced to differentiate into myotubes with or without Piezo1 agonist Yoda1 in vitro. Treatment with the Piezo1 agonist Yoda1 significantly promoted MYHC-positive myotube formation of MuSCs from RCT patients, indicating improved myogenic differentiation ability (Fig. 6a and b). Consistently, gene expression analysis also revealed upregulated expression of myogenic marker genes (e.g., MYH1, MYOG, MCK) upon Yoda1 treatment (Fig. 6c). These results further supported the notion that activating Piezo1 could improve myogenic differentiation ability of MuSCs after RCT.

To further investigate the effects of Yoda1 in vivo, 12-week-old mouse RCT models were firstly established and randomly divided into two groups. Two weeks later, the mice in Yoda1 group were treated with 5 μmol/kg Yoda1 for two weeks (Intraperitoneal injection, every twice day), while the mice in control group were injected with equal volume of vehicle (DMSO diluted in 5 % ethanol) (Fig. 7a). Four weeks after establishment of RCT model, subsequent analyses (gait analysis, treadmill and muscle sample assessment) were conducted.

Immunostaining for Laminin was performed to assess cross-sectional area of myofibers in supraspinatus muscles (Fig. 7b). The RCT model treated with Yoda1 showed significantly larger cross-sectional area of myofibers when compared to untreated controls (Fig. 7c). Thus, these data indicated that activating Piezo1 could prevent muscle degeneration after RCT. To further investigate the recue effects of Yoda1, shoulder function was subsequently evaluated. Gait analysis experiments demonstrated an increase in

step length, indicating enhanced muscle function and mobility after Yoda1 treatment (Fig. 7d). Furthermore, treadmill endurance tests showed improved exercise capacity and delayed exhaustion in mice treated with Yoda1, highlighting enhanced muscle performance and shoulder function (Fig. 7e and f).

Taken together, Yoda1 treatment could alleviate the muscle degeneration and enhance the shoulder function in RCT model.

3. Discussion

The current study revealed that there was significantly decreased expression level of PIEZO1 and impaired myogenic potential in MuSCs after RCT. Reduced expression of PIEZO1 impaired the myogenesis of MuSCs by inhibiting the ERK/MAPK pathways. Furthermore, selective PIEZO1 activator Yoda1 had the potential to alleviate muscle degeneration and improve shoulder function following RCT. This study emphasized the role of PIEZO1 in the myogenesis of MuSCs and suggests that activating PIEZO1 could be a potential non-surgical treatment option to reduce muscle degeneration after RCT.

Rotator cuff tear (RCT) is a prevalent issue in orthopedic surgery, often resulting in chronic shoulder pain and disability [11]. Although surgical repair is the primary treatment for RCT, the re-tear rate remains notably high despite advanced surgical techniques [12]. Irreversible muscular degeneration following RCT is a major factor contributing to poor surgical outcomes [13,14].
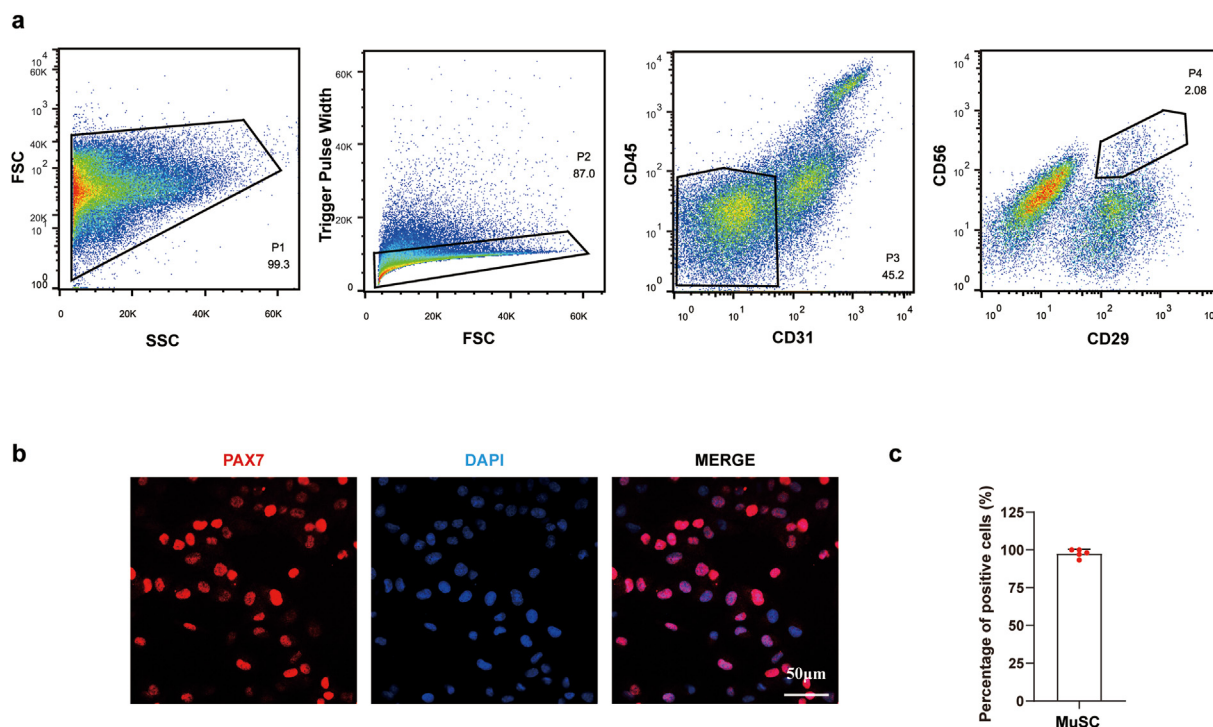
Fig. 2. Purification of human muscle stem cells by fluorescence-activated cell sorting. a. Diagrams of fluorescence-activated cell sorting for human muscle stem cells. b and c. Immunofluorescence staining and statistical analysis of PAX7 for purified human muscle stem cells from supraspinatus muscle tissues (n = 5). Scale bar, 50 μm.

However, addressing this issue in clinical practice is challenging due to an incomplete understanding of the mechanisms underlying muscle degeneration. Therefore, it is crucial to investigate the mechanisms of muscle degeneration after RCT.

MuSCs are a heterogeneous stem cell population primarily contributing to postnatal skeletal muscle growth, regeneration, and repair. These cells are activated by external stimuli to proliferate, differentiate, and fuse into damaged myofibers [5–7]. The poor clinical outcomes of RCT have been attributed to the inability of rotator cuff muscle to properly recover in response to restored functional loading [15]. Normally, muscle regeneration and hypertrophy depend on MuSCs to add fiber volume and sarcomeres. However, the limited recovery of rotator cuff muscle following repair suggests a potential deficit with MuSCs. Thus, the current study was performed to investigate the potential pathological changes and detailed molecular mechanism underlying the myogenesis of MuSCs after RCT. Schubert et al. found reduced myogenic and increased adipogenic capacity of MuSCs from rotator cuff muscles when compared with gastrocnemius muscle in mouse model [6]. Meyer et al. isolated skeletal muscle progenitor cells and found significantly reduced proliferative ability which could impair regenerative capacity in torn rotator cuff [16]. These studies indicated the potential deficits of MuSCs in rotator cuff, while in-depth investigation is still waiting to be performed. In current study, single cell landscape of supraspinatus muscle cells after RCT indicated the potential impaired ability of myogenesis for MuSCs. Purified MuSCs were then confirmed by PAX7 staining and impaired myogenic differentiation was determined in vitro. Thus, deficits of myogenesis of MuSCs isolated from supraspinatus muscles after RCT was robustly demonstrated in this study.

The current study also found that PIEZO1 was downregulated in MuSCs in supraspinatus muscles after RCT, which impaired myogenic differentiation potential of these cells both in vivo and in vitro. Given that RCT inevitably disrupts the biomechanical microenvironment of rotator cuff muscles, it is reasonable to conclude that RCT contributes to altered biological effects through the mechanosensory protein PIEZO1 [17]. PIEZO1 is a well-known mechanosensory protein integral in transducing mechanical signals and mediating physiological activities [7]. Peng et al. have demonstrated that expression of PIEZO1 would be increased during in vitro myogenesis of MuSCs, indicating the potential crucial role of PIEZO1 in myoblast fusion [18]. It has also been reported that activation of PIEZO1 could ameliorate the regenerative defects of dystrophic muscles by adjusting states of MuSCs [7]. In addition, knockdown of PIEZO1 could significantly suppress myoblast fusion and lead to smaller myotubes, which was accompanied by significant decreased expression of fusogenic marker Myomaker [19]. Thus, PIEZO1 plays a crucial role in regulating physiology of skeletal muscle by targeting MuSCs. However, the detailed role of PIEZO1 in muscle degeneration after RCT still remains unclear. It is worth noting that it was the first study to find the decreased expression of PIEZO1 in MuSCs after RCT, which also elucidated the direct regulatory role of PIEZO1 on the myogenesis of MuSCs, shedding light on the mechanism behind muscular degeneration after RCT. Thus, potential therapeutic effects of specific PIEZO1 channel agonist Yoda1 was investigated for muscle degeneration after RCT. Myogenic differentiation inability, muscular atrophy and shoulder function were significantly improved after treatment of Yoda1 in RCT model. Therefore, activation of PIEZO1 channels could be a potential non-surgical treatment option to reduce muscle degeneration after RCT.

The current study added more knowledge to the pathophysiology for rotator cuff degeneration in RCT patients. Since all the patients enrolled were the elderly aged from fifty to seventy years old in current study, ageing factor was excluded in the finding of current study. Furthermore, PIEZO1, the well-known mechanosensory protein integral in transducing mechanical signals [7], was identified as the key gene to bridge the reduced mechanical
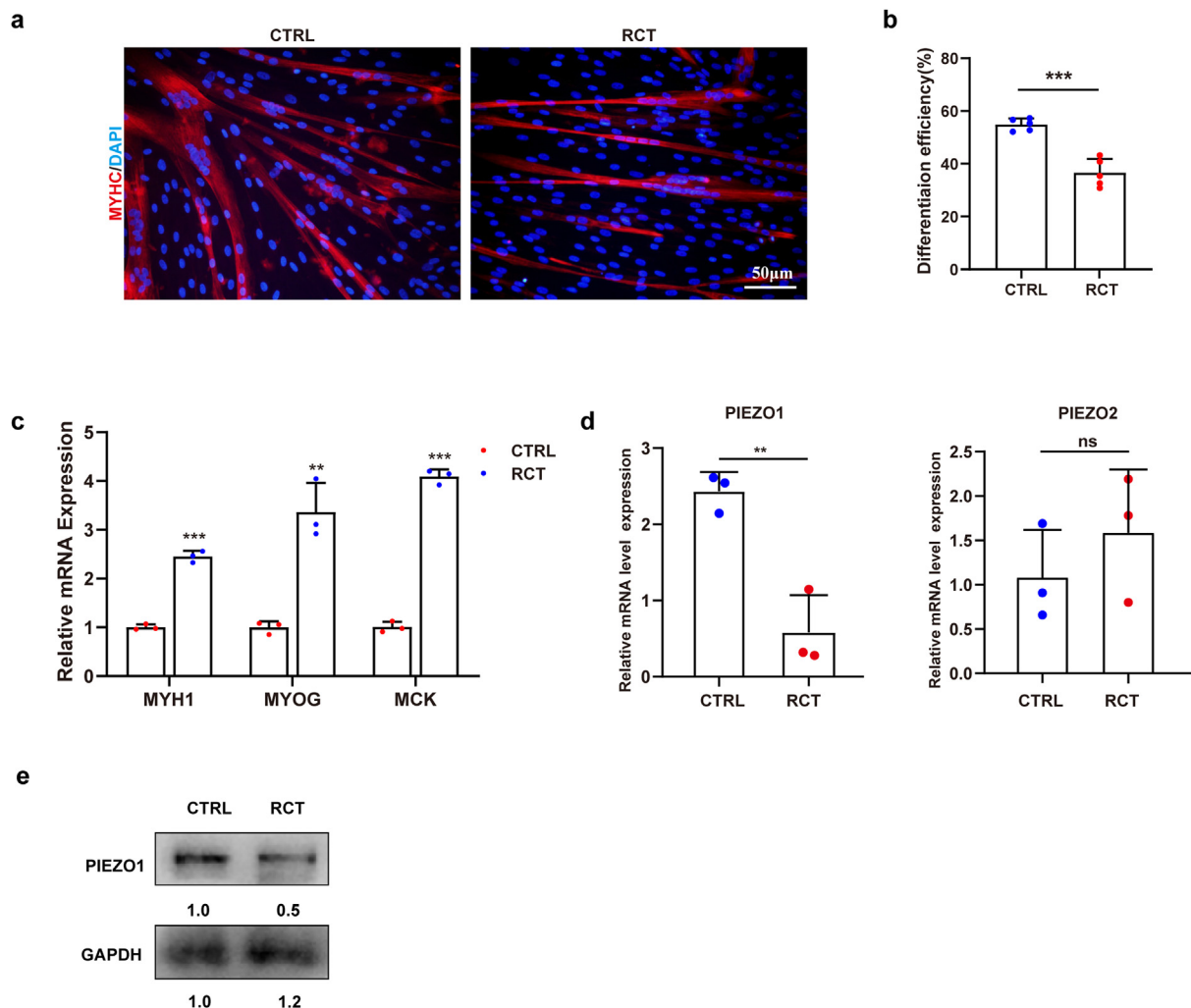
Fig. 3. There were decreased myogenic differentiation ability and reduced expression of PIEZO1 in supraspinatus MuSCs after rotator cuff tears. a and b. Immunofluorescence staining and statistical analysis of MYHC for myogenically differentiated human MuSCs from healthy supraspinatus muscle (CTRL) or supraspinatus muscle with rotator cuff tears (RCT) (n = 5). Scale bar, 100 μm. c. The mRNA expression of MYH1, MYOG, and MCK of myogenically differentiated MuSCs in CTRL group and RCT group (n = 3). d. The mRNA expression of PIEZO1 and PIEZO2 of MuSCs in CTRL group and RCT group (n = 3). e. The protein levels of PIEZO1 in CTRL group and RCT group. ** indicated $p < 0.01$, ***indicated $p < 0.001$.

stimulation and impaired myogenesis. Thus, the myogenesis defects of MuSCs were more likely to be due to the mechanical detachment in RCT, which was also consistent with the pathophysiology of the widely used mouse RCT model [12,14] in current study. It seems reasonable that the mechanical unloading caused by RCT decreased the expression of PIEZO1 in MuSCs, while the impaired PIEZO1-MAPK axis suppressed the myogenesis of MuSCs. Then rotator cuff degeneration occurred due to dysfunction of MuSCs, which in verse contributed to poor clinical outcomes and failed rotator cuff repair. However, further investigations should be performed to detail this theory.

In conclusion, there was significantly decreased expression level of PIEZO1 and impaired myogenic potential in MuSCs after RCT. Reduced expression of PIEZO1 impaired the myogenesis of MuSCs by inhibiting the ERK/MAPK pathways. Furthermore, selective PIEZO1 activator Yoda1 had the potential to alleviate muscle degeneration and improve shoulder function following RCT. This study emphasized the role of PIEZO1 in the myogenesis of MuSCs and suggested that activating PIEZO1 could be a potential non-surgical treatment option to reduce muscle degeneration after RCT.

4. Methods and materials

4.1. Animal and human samples

All animal-related experimental procedures were conducted in accordance with the guidelines approved by the Animal Ethics and Welfare Committee of the local institution (Approval NO. IACUC-FPH-PZ-20240528 and K2024-01-011). Wild-type male mice (C57BL/6, twelve weeks old) and Piezo1 f/f mice were obtained from Gem Pharmatech (Nanjing, China). Pax7-CreERT2 mice were sourced from Jackson Laboratory. To induce conditional gene knockout, mice were administered 100 μL of 10 mg/mL tamoxifen (ABCONE, Cat# T56488) daily for one week, starting in the three weeks old. Then the collection of muscle specimen from MuSCs-specific Piezo1 KO mouse for MuSC separation was performed at the age of six weeks old. The RCT animal models were established at twelve weeks old following previously described protocols [12,14]. In brief, the tendons of the supraspinatus and infraspinatus muscles in the right shoulder were completely transected near the humeral head. For the left shoulder, a sham surgery was performed without tendon detachment to serve as a control.
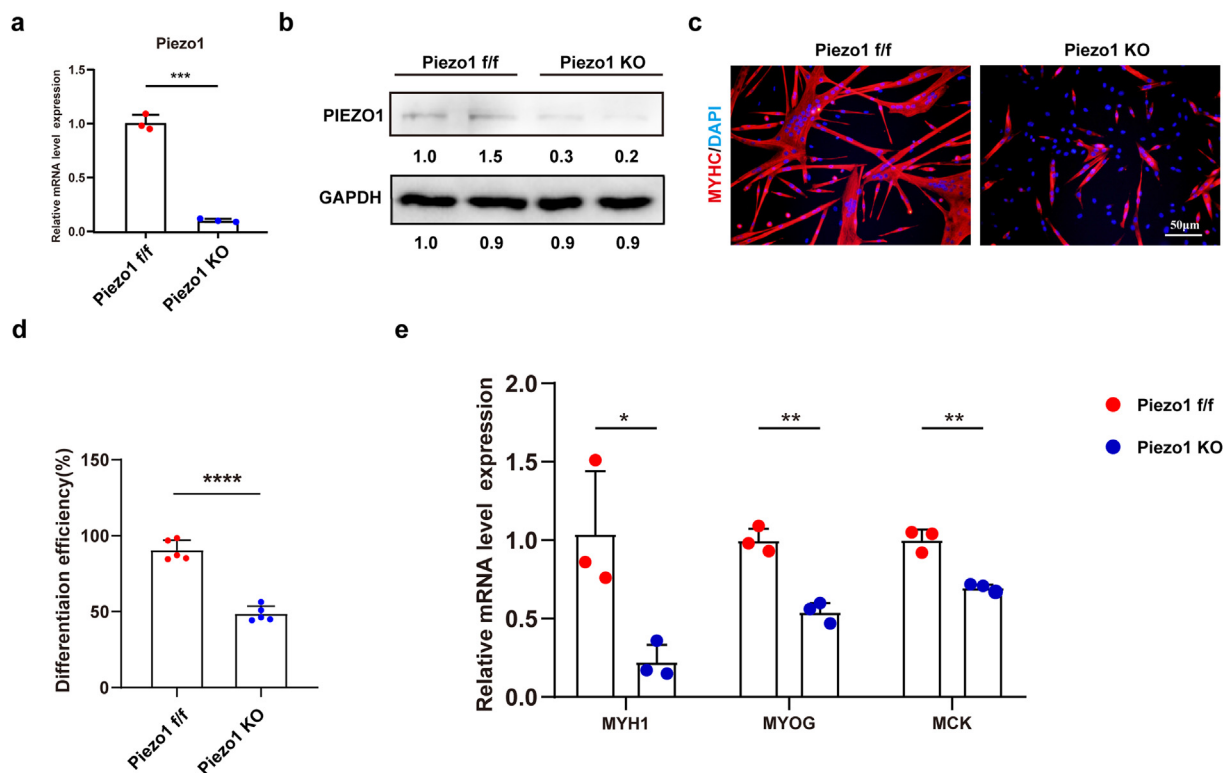
Fig. 4. Ablation of Piezo1 in MuSCs led to decreased myogenic differentiation ability. a. The mRNA expression of Piezo1 in Piezo1 flox/flox (f/f) MuSCs and Piezo1 knockout (KO) MuSCs (n = 3). b. The protein levels of Piezo1 in Piezo1 flox/flox (f/f) MuSCs and Piezo1 knockout (KO) MuSCs. c and d. Immunofluorescence staining and statistical analysis of MYHC for myogenically differentiated Piezo1 f/f MuSCs and Piezo1 KO MuSCs (n = 5). Scale bar, 50 μm. e. The mRNA expression of MYH1, MYOG, and MCK of myogenically differentiated Piezo1 f/f MuSCs and Piezo1 KO MuSCs (n = 3). *indicated p < 0.05, ** indicated p < 0.01, ***indicated p < 0.001, ****indicated p < 0.0001.

Muscle samples, both with and without RCT, were obtained from patients undergoing arthroscopic repair, total reverse shoulder replacement, or tendon transfer surgery. All the patients enrolled were the elderly aged from fifty to seventy years old. The collection of these samples did not introduce any additional complications for the patients. Informed consent was obtained and signed by all participants.

4.2. Isolation of muscle stem cells

The digestion procedure for skeletal muscle was carried out as previously described [20]. Fresh muscle tissue was mechanically minced and digested with collagenase II (Worthington Biochemical, 700–800 U/ml, Cat# LS004177) for 1 h. Subsequently, the muscle fragments were treated with a combination of collagenase II (70–80 U/ml) and Dispase (Life Technologies, Cat# 17105041, 11 U/ml) for 30 min. The resulting single-cell suspension was filtered through 70 μm and 40 μm strainers (BD Falcon). Red blood cells were eliminated using a red cell lysis buffer (Thermo Fisher Scientific, Cat# 00-433-57).

For the isolation of human muscle stem cells, the single-cell suspension was stained with Percp/cy5.5 anti-human CD31 (BioLegend, Cat# 30313), Pecy5 anti-human CD45 (BD Biosciences, Cat# 555484), AF-488 anti-human CD29 (BioLegend, Cat#303016) and PE anti-human CD56 (BioLegend, Cat#304606) for 45 min with agitation. The subgroup of CD31-CD45-CD56$^+$CD29$^+$ cells was subsequently sorted using a BD Influx sorter (9).

For the isolation of mice muscle stem cells, the mice mononuclear cells were stained with AF700-anti-mouse Sca-1, PerCP/Cy5.5-anti-mouse CD31, PerCP/Cy5.5-anti-mouse CD45, FITC anti-mouse CD34, APC-anti-mouse Integrin α7+), the CD31-CD45-SCA-1-CD34+Integrinα+ subcluster cells were isolated (BD Biosciences).

4.3. Cell culture, treatment, and differentiation

Primary human and mouse muscle stem cells were cultured in F10 basal medium (Gibco, cat#11550043) containing 20 % FBS (Gibco, Cat# 10-013-CV), 2.5 ng/mL bFGF (R&D, Cat# 233-FB-025), and 1 % penicillin-streptomycin (Gibco, Cat# 15140-122). To investigate the physiological role of PIEZO1 in the myogenesis of muscle stem cells and its related mechanisms, 2.5 μM Yoda1 (MCE, Cat#HY-18723), 2.5 μM GsMTx4 (MCE, Cat#HY-P1410), 5 μM TBHQ (MCE, Cat#HY-100489), and 1 μM U-0126 (MCE, Cat#HY-12031A) were applied. For the myogenic induction experiment, muscle stem cells were treated with a myogenic induction medium comprising high-glucose DMEM (Gibco, Cat# 12100-046) supplemented with 2 % horse serum, and 1 % penicillin-streptomycin. Induction of myogenesis was performed for 2 days for mouse MuSCs and 4 days for human MuSCs.

4.4. Single-cell RNA sequencing

Single-cell suspensions were isolated from discarded supraspinatus muscles of patients with or without RCT. The single-cell RNA sequencing procedure and subsequent analysis were conducted as previously described. Live cells were stained with propidium iodide (Sangon Biotech, Cat# E607328) and Hoechst (Sangon Biotech, Cat# A601112), followed by FACS sorting. Chromium Single Cell 3' Reagent Kits (10X Genomics, Cat# 1000121-
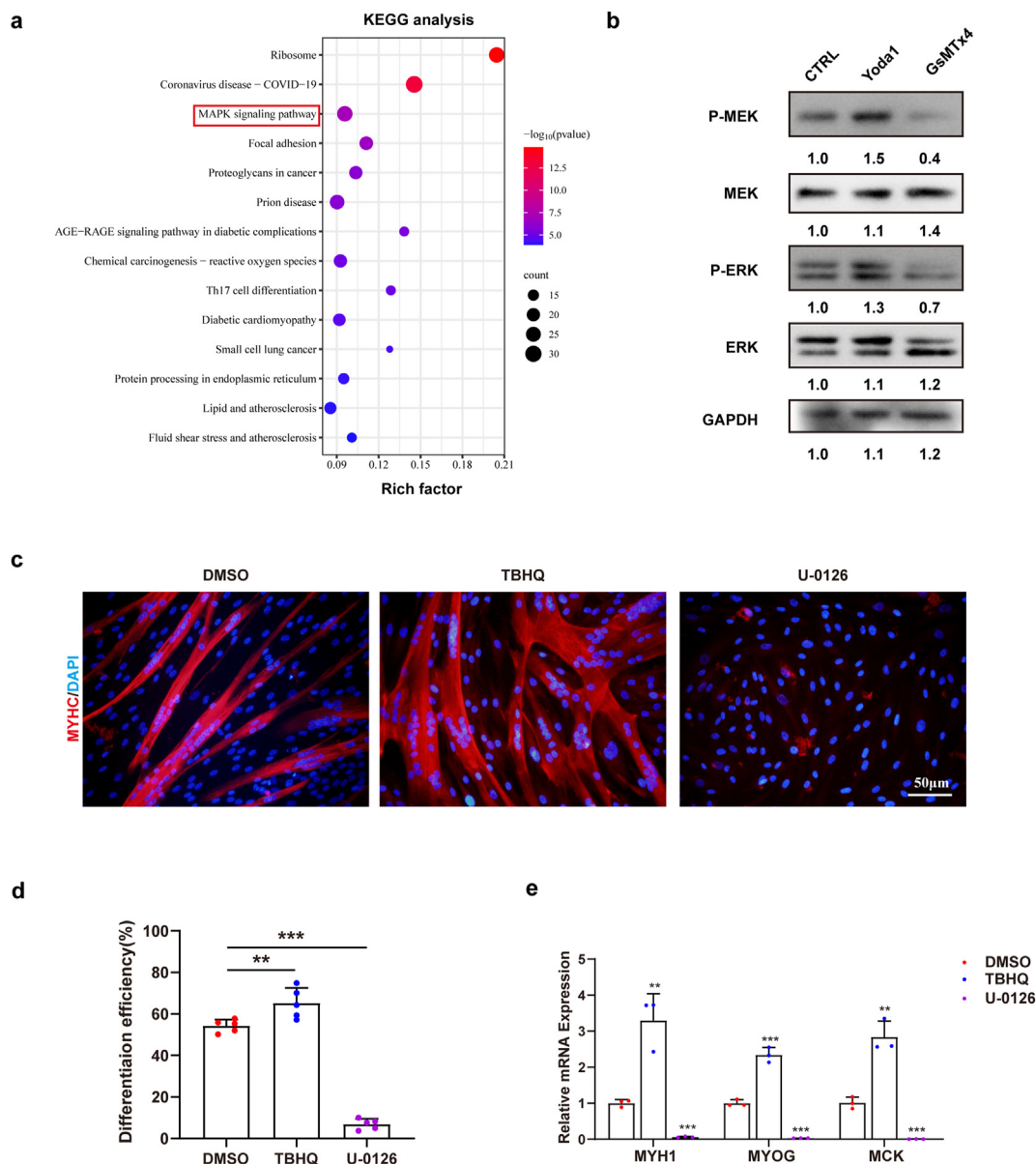
Fig. 5. PIEZO1 regulated myogenic differentiation of MuSCs by MAPK pathways. a. KEGG enrichment analysis of differently expressed genes between human MuSCs from healthy supraspinatus muscle (CTRL) or supraspinatus muscle with rotator cuff tears (RCT). b. The protein levels of MEK, p-MEK, ERK, p-ERK, and GAPDH in MuSCs from healthy supraspinatus muscles after treatment with PIEZO1 agonist Yoda1 or inhibitor GsMTx4. c and d. Immunofluorescence staining and statistical analysis of MYHC for myogenically differentiated healthy MuSCs with treatment of MAPK signaling agonist TBHQ or inhibitor U0126 (n = 5). Scale bar, 50 μm. e. The mRNA expression of MYH1, MYOG, and MCK of myogenically differentiated healthy MuSCs with treatment of MAPK signaling agonist TBHQ or inhibitor U0126 (n = 3). ** indicated p < 0.01, ***indicated p < 0.001.

1000157) were used for library construction, and sequencing was performed on the Illumina Novaseq 6000 platform (Illumina). Data analysis was carried out on a bioinformatics platform (Majorbio, China). Cells with fewer than 200 genes, more than 8000 genes, or over 16 % mitochondrial genes were excluded from the analysis, resulting in a dataset of 22,858 cells for subsequent analysis. Cell clustering was carried out using the "FindClusters" function with a resolution set to 0.15, and dimensionality reduction was achieved via the "RunUMAP" function. Ultimately, 8 distinct clusters of cells were identified. To determine cell types, the clusters were analyzed through the "FindClusters" function. Marker genes specific to each cluster were identified with the "FindAllMarkers" function, including only those with p values below 0.05 and |logFC| greater than 0.25. Cell types were then assigned based on the expression of established marker genes.

4.5. Immunofluorescent staining

Fixed cells and muscle slices were permeabilized by 0.5 % TritonX-100 for 30 min at room temperature, and subsequently blocked with 1 % BSA (Beyotime Biotechnology, cat#ST023) for 1 h. Primary anti-PAX7 (Developmental Studies Hybridoma bank, 1:100), anti-MyHC (Millipore, cat#05-716), Laminin (Abcam, Cat#11575) were incubated overnight at 4 °C. Then, the secondary antibodies, alexa Fluor goat anti-mouse 594 and alexa Fluor goat anti-rabbit 488 (Invitrogen, 1:100) were incubated for 1 h. Finally, the 4, 6-diamidino-2-phenylindole (DAPI, Vector Laboratories, cat#H-1200) was applied for marking the nucleus of cells. Evaluation of myogenic differentiation efficiency was performed to calculate the percentage of nuclei within MyHC labeled myotube (nuclei within MyHC labeled myotube/total nuclei).
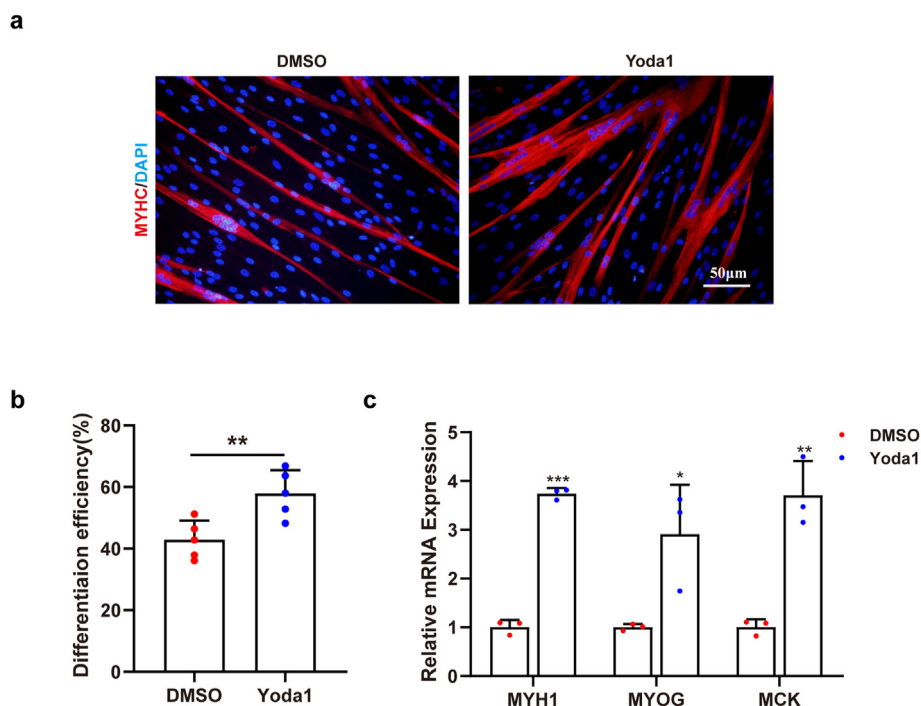
Fig. 6. PIEZO1 agonist Yoda1 rescued myogenic differentiation deficit in MuSCs after rotator cuff tears. a and b. Immunofluorescence staining and statistical analysis of MYHC for myogenically differentiated MuSCs after RCT with or without treatment of PIEZO1 agonist Yoda1 (n = 5). Scale bar, 50 μm. c. The mRNA expression of MYH1, MYOG, and MCK of myogenically differentiated MuSCs after RCT with or without treatment of PIEZO1 agonist Yoda1 (n = 3). *indicated p < 0.05, ** indicated p < 0.01, ***indicated p < 0.001.
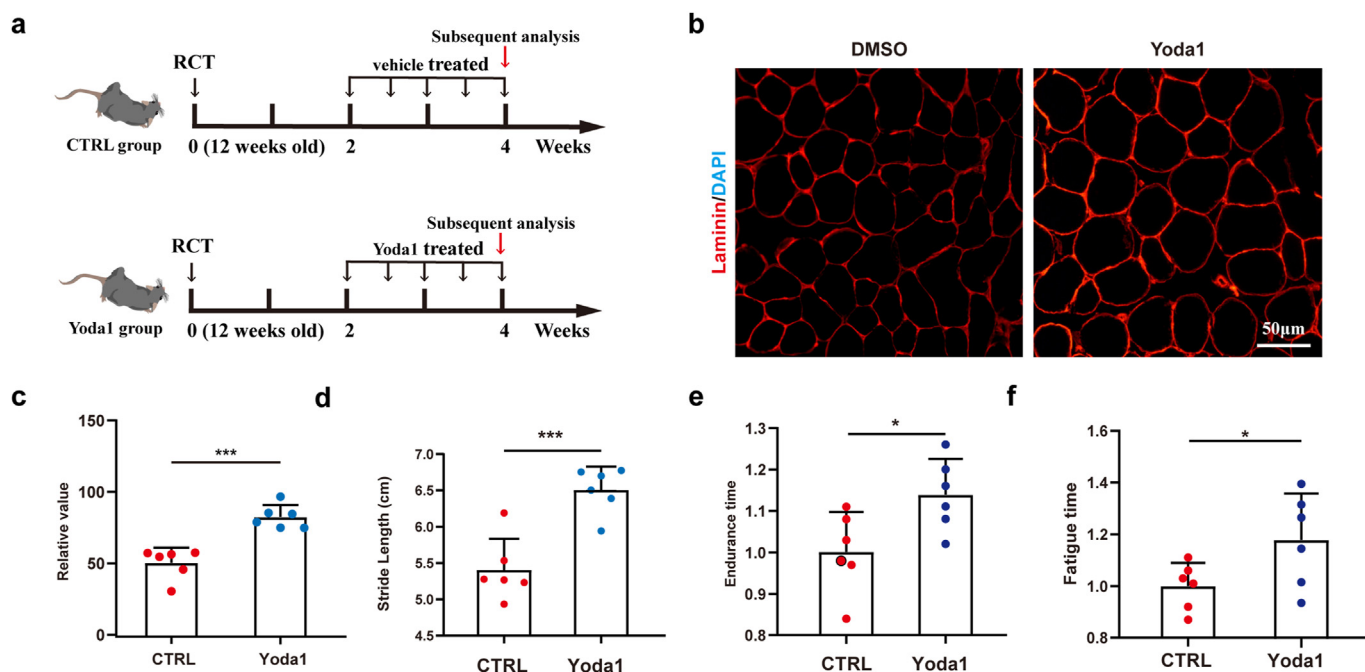

Fig. 7. PIEZO1 agonist Yoda1 could alleviate the muscle degeneration and enhance the shoulder function in RCT model. a. The schematic diagram of animal experimental design. b and c. Immunofluorescence staining of Laminin and statistical analysis of cross-sectional area of myofibers in supraspinatus muscles with or without treatment of PIEZO1 agonist Yoda1 after rotator cuff tears (n = 6). Scale bar, 50 μm. d. The gait analysis for rotator cuff tears models with or without treatment of PIEZO1 agonist Yoda1 after rotator cuff tears (n = 6). e and f. Fatigue running time for rotator cuff tears models with or without treatment of PIEZO1 agonist Yoda1 after rotator cuff tears (n = 6). *indicated p < 0.05, ***indicated p < 0.001.

4.6. RNA isolation and cDNA synthesis

Total RNA was isolated using the EZ-press RNA Purification Kit (EZBioscience, Cat# B0004DP) according to the manufacturer's instructions. One microgram of RNA was reverse transcribed into cDNA using MuLV reverse transcriptase (NEB, Cat# M0253L). The cDNA products served as templates for real-time PCR reactions using Genious 2X SYBR Green Fast qPCR Mix (Abclonal, Cat#

RK21205) in the CFX96 real-time PCR system. The primers were provided by Tsingke Biotech and the sequences were listed below:

Human GAPDH-F 5′-CAAGGCTGAGAACGGGAAGC-3′;
Human GAPDH-R 5′-AGGGGGCAGAGATGATGACC-3′;
Human MYH1-F 5′-GGGAGACCTAAAATTGGCTCAA-3′;
Human MYH1-R 5′-TTGCAGACCGCTCATTTCAAA-3′;
Human MYOG-F 5′-GCTCAGCTCCCTCAACCA-3′;
Human MYOG-R 5′-GCTGTGAGAGCTGCATTCG-3′;
Human CKM-F 5′-ATGCCATTCGGTAACACCCAC-3′;
Human CKM-R 5′-GCTTCTTGTAGAGTTCAAGGGTC-3′;
Human-PIEZO1-F 5′-CAGGCCTATGAGGAGCTGTC-3′;
Human-PIEZO1-R 5′-TTGTAGAGCTCCCGCTTCAT-3′;
Human-PIEZO2-F 5′-GCCCAACAAAGCCAGTTGAA-3′;
Human-PIEZO2-R 5′-GGGCTGATGGTCCACAAAGA-3′;
Mouse Gapdh-F 5′-ACCCAGAAGACTGTGGATGG-3′;
Mouse Gapdh-R 5′-ACACATTGGGGGTAGGAACA-3′;
Mouse Myh1-F 5′-GCGAATCGAGGCTCAGAACAA-3′;
Mouse Myh1-R 5′-GTAGTTCCGCCTTCGGTCTTG-3′;
Mouse MyoG-F 5′-GAGACATCCCCCTATTTCTACCA-3′;
Mouse MyoG-R 5′-GCTCAGTCCGCTCATAGCC-3′;
Mouse Mck-F 5′-AGACAAGCATAAGACCGACCT-3′;
Mouse Mck-R 5′-AGGCAGAGTGTAACCCTTGAT-3′;
Mouse-Piezo1-F 5′-CCTGTTACGCTTCAATGCTCT-3′;
Mouse-Piezo1-R 5′-GTGTAGGCATATCTGAAAGGCAA-3'.

4.7. Western blot analysis

Total proteins were extracted using Western and IP lysis buffer (Beyotime, Cat# P0013). The proteins were separated by electrophoresis on polyacrylamide gels and transferred to nitrocellulose membranes. Following 1-h blocking with 5 % BSA, primary antibodies were incubated overnight at 4 °C. The primary antibodies used in this study included anti-GAPDH (Cell Signaling Technology, Cat# 5174), anti-ERK1/2 (Cell Signaling Technology, Cat# 4695T), anti-phospho-ERK1/2 (Cell Signaling Technology, Cat# 4370T), anti-MEK1/2 (Abclonal, Cat# A4868), Piezo1 (Proteintech, Cat# 15939-1-AP) and anti-phospho-MEK1/2 (Cell Signaling Technology, Cat# 9154T). After washing the membranes three times with $1 \times$ TBST, an HRP-conjugated secondary antibody, anti-rabbit IgG (Santa Cruz, Cat# sc-2357), was incubated for 1 h. Visualization of specific bands was achieved using LumiQ ECL liquid (ShareBio, Cat# SBWB012) and GelDoc XR system (Bio-Rad).

4.8. Gait analysis

Gait analysis of mice with RCT was conducted using the Noldus Catwalk System, as previously detailed [14]. Prior to the formal experiment, mice underwent tunnel navigation training with speeds more than 10 m/min. This experiment recorded various gait parameters, including stride length, stance width, and paw area at peak stance. Stride length indicates shoulder abduction in mice, stance width reflects limb load-bearing capacity, and paw area at peak stance indicates chronic pain. Assessment of these parameters allows for evaluation of the functional consequences of shoulder in RCT mice.

4.9. Treadmill analysis

Treadmill analysis was performed using the Zll-PT/5 S treadmill apparatus, as previously outlined [12]. Mice were familiarized with the treadmill apparatus before formal experiments. In the endurance experiment, mice ran on the treadmill at a speed of 20 m/min. In exhaustion experiments, the initial speed was set at 16 m/min and increased by 2 m/min every 3 min. Termination criteria for both tests were met when mice ceased running for 10 s, despite electrical stimulus.

4.10. Statistical analysis

The reliability and reproducibility of the results were described in the figure legends. To minimize bias, the operator remained blinded to group information during data analysis and evaluation. Randomization was conducted using SPSS software. Experimental data were presented as mean $\pm$ SD. Statistical differences between groups were evaluated using Student's t-test or one-way ANOVA in GraphPad Prism 8 software. A significance threshold of $P < 0.05$ was applied.

Consent for publication

All the authors consent to the publication of the current study.

Availability of supporting data

The data presented in this study are available on request from the corresponding author (accurately indicate status).

Ethics statement

The study was approved by local ethical Committee (Approval NO. K2024-01-011) and Approval No. IACUC-FPH-PZ-20240528 [0007]).

Authors' contributions

TW and SF designed the study, collected the experimental data and wrote the original draft. TW and RZ conducted the image analysis, statistical analysis, and wrote the original draft. MW, RB, HJ and YX designed the study, reviewed and edited the manuscript. RZ, FL and ZH administrated the project and edited the manuscript.

Declaration of competing interest

The authors have declared no conflict of interest.

Acknowledgement

References

[1] Sun Y, et al. Small subchondral drill holes improve marrow stimulation of rotator cuff repair in a rabbit model of chronic rotator cuff tear. Am J Sports Med 2020;48:706—14. https://doi.org/10.1177/0363546519896350.

[2] Galatz LM, Ball CM, Teefey SA, Middleton WD, Yamaguchi K. The outcome and repair integrity of completely arthroscopically repaired large and massive rotator cuff tears. J Bone Joint Surg Am 2004;86:219—24. https://doi.org/10.2106/00004623-200402000-00002.

[3] Hein J, Reilly JM, Chae J, Maerz T, Anderson K. Retear rates after arthroscopic single-row, double-row, and suture bridge rotator cuff repair at a minimum of 1 Year of imaging follow-up: a systematic review. Arthroscopy 2015;31: 2274—81. https://doi.org/10.1016/j.arthro.2015.06.004.

[4] Tang X, et al. The treatment of muscle atrophy after rotator cuff tears using electroconductive nanofibrous matrices. Regen Eng Transl Med 2021;7:1—9. https://doi.org/10.1007/s40883-020-00186-8.

[5] Shao X, et al. The asymmetrical ESR1 signaling in muscle progenitor cells determines the progression of adolescent idiopathic scoliosis. Cell Discov 2023;9:44. https://doi.org/10.1038/s41421-023-00531-5.

[6] Schubert MF, Noah AC, Bedi A, Gumucio JP, Mendias CL. Reduced myogenic and increased adipogenic differentiation capacity of rotator cuff muscle stem cells. J Bone Jt Surg Am Vol 2019;101:228—38. https://doi.org/10.2106/JBJS.18.00509.

[7] Ma N, et al. Piezo1 regulates the regenerative capacity of skeletal muscles via orchestration of stem cell morphological states. Sci Adv 2022;8:eabn0485. https://doi.org/10.1126/sciadv.abn0485.

[8] Sousa-Victor P, García-Prat L, Muñoz-Cánoves P. Control of satellite cell function in muscle regeneration and its disruption in ageing. Nat Rev Mol Cell Biol 2022;23:204—26. https://doi.org/10.1038/s41580-021-00421-2.

[9] Nakamichi R, et al. The mechanosensitive ion channel PIEZO1 is expressed in tendons and regulates physical performance. Sci Transl Med 2022;14: eabj5557. https://doi.org/10.1126/scitranslmed.abj5557.

[10] Greenspoon JA, Petri M, Warth RJ, Millett PJ. Massive rotator cuff tears: pathomechanics, current treatment options, and clinical outcomes. J Shoulder Elbow Surg 2015;24:1493—505. https://doi.org/10.1016/j.jse.2015.04.005.

[11] Agha O, et al. Rotator cuff tear degeneration and the role of fibro-adipogenic progenitors. Ann N Y Acad Sci 2020;1490:13—28. https://doi.org/10.1111/nyas.14437.

[12] Zhou H, et al. Metformin mitigates adipogenesis of fibro-adipogenic progenitors after rotator cuff tears via activating mTOR/ULK1-mediated autophagy. Am J Physiol Cell Physiol 2024;326:C1590—603. https://doi.org/10.1152/ajpcell.00034.2024.

[13] Saveh Shemshaki N, et al. Muscle degeneration in chronic massive rotator cuff tears of the shoulder: addressing the real problem using a graphene matrix. Proc Natl Acad Sci U S A 2022;119:e2208106119. https://doi.org/10.1073/pnas.2208106119.

[14] Lin X, et al. Suppressed Akt/GSK-3beta/beta-catenin signaling contributes to excessive adipogenesis of fibro-adipogenic progenitors after rotator cuff tears. Cell Death Dis 2023;9:312. https://doi.org/10.1038/s41420-023-01618-4.

[15] Gladstone JN, Bishop JY, Lo IK, Flatow EL. Fatty infiltration and atrophy of the rotator cuff do not improve after rotator cuff repair and correlate with poor functional outcome. Am J Sports Med 2007;35:719—28. https://doi.org/10.1177/0363546506297539.

[16] Meyer GA, et al. Muscle progenitor cell regenerative capacity in the torn rotator cuff. J Orthop Res 2015;33:421—9. https://doi.org/10.1002/jor.22786.

[17] Ruderman L, et al. Histologic differences in human rotator cuff muscle based on tear characteristics. J Bone Joint Surg Am 2022;104:1148—56. https://doi.org/10.2106/JBJS.21.01304.

[18] Peng Y, et al. Mechano-signaling via Piezo1 prevents activation and p53-mediated senescence of muscle stem cells. Redox Biol 2022;52:102309. https://doi.org/10.1016/j.redox.2022.102309.

[19] Ortuste Quiroga HP, et al. Fine-tuning of Piezo1 expression and activity ensures efficient myoblast fusion during skeletal myogenesis. Cells 2022;11. https://doi.org/10.3390/cells11030393.

[20] Shao X, et al. Human muscle-derived cells are capable of tenogenic differentiation and contribution to tendon repair. Am J Sports Med 2023;51:786—97. https://doi.org/10.1177/03635465221147486.